

## On the Equilibrium Diagram of Manganese and Carbon Alloy

著者	ISOBE Mitsutake
journal or publication title	Science reports of the Research Institutes, Tohoku University. Ser. A, Physics, chemistry and metallurgy
volume	3
page range	468-490
year	1951
URL	<a href="http://hdl.handle.net/10097/26457">http://hdl.handle.net/10097/26457</a>

# On the Equilibrium Diagram of Manganese and Carbon Alloy\*

Mitsutake ISOBE

*The Research Institute for Iron, Steel and Other Metals*

(Received June 15, 1951)

## Synopsis

The equilibrium diagram of manganese and carbon system was studied with distilled manganese and sugar charcoal.

In this alloy series, seven kinds of solid solutions,  $\alpha$ ,  $\beta$ ,  $\gamma$ ,  $\delta$ -manganese solid solutions,  $\alpha$ C,  $\beta$ C and  $\gamma$ C solid solutions, existed and their existing regions were clarified. On solidification, three kinds of peritectic reactions occurred at 1235°, 1260° and 1340°C, respectively, and in the solid state, two kinds of peritectoid reactions existed at 857°C and 1010°C, respectively, and two kinds of eutectoid reactions at 820°C and 950°C, respectively.

$\alpha$ -Manganese dissolved about 0.3 per cent of carbon at room temperature, and 1.0 per cent of carbon at eutectoid temperature 820°C. Maximum solubility of carbon in  $\beta$ -manganese was 0.05 per cent at 857°C.  $\gamma$ -manganese dissolved a comparatively large amount of carbon, say, 2.95 per cent of carbon at 1260°C. Solubility of carbon in  $\delta$ -manganese at 1235°C was 0.12 per cent.

$\alpha$ C solid solution was a new phase recognized first by the present writer. It contained more than 7.0 per cent of carbon, and was conceived to be manganese carbide  $Mn_2C$  (9.85% C) with dissolved manganese. Manganese carbide  $Mn_3C$  which had been supposed to exist, was not recognized in the present research.  $\beta$ C solid solution was observed in the alloys containing more than 3.05 per cent of carbon at high temperatures. Quenched  $\beta$ C solid solution was comparatively stable at room temperature and the so-called weathering phenomenon scarcely occurred under this condition.

The  $\gamma$ C solid solution produced by the peritectoid reaction at 1010°C was also found newly by the present writer, the composition of which seemed to be about  $Mn_4C$  (5.18% C). This phase existed at room temperature in the range from 4.3 to 4.6 per cent of carbon.

## I. Introduction

Although many studies<sup>(1)(2)(3)</sup> have been carried out on the alloy system of manganese and carbon, the equilibrium diagram has not been completed. The

\* The 647th report of the Research Institute for Iron, Steel and Other Metals.

(1) A. Stadel, *Metallurgie*, **5** (1908), 260.

(2) O. Ruff and W. Bormann, *Zeit. anorg. Chem.*, **88** (1914), 365.

(3) K. Kido, *Sci. Rep., Tohoku Imp. Univ.*, **9** (1920), 305.

diagram of R. Vogel and W. Doring<sup>(4)</sup> is the only one showing a comparatively deep investigation, though not perfect, especially, at high carbon regions.

It was probably due to the extraordinary difficulties in carrying out experiments that a satisfactory diagram has not been obtained. For example, high manganese alloys attack the refractory vessels during melting; the preparation of sample is very difficult because of the brittleness; the volatilization and oxidation of both manganese and carbon in high manganese and high carbon alloys easily take place at high temperatures; the sample is easily disintegrated in short time by the weathering in atmosphere, and so forth. Hence, in the present investigation, the samples were all stored in vacuum vessels, or in case the samples were frequently taken out in atmosphere for examinations, they were stored in the vessels containing an unhydrated oil. In spite of such discretions, however, the samples were gradually disintegrated with the lapse of time.

Extending over several years, the present writer studied alloys of iron-manganese-carbon series, and after experienced many difficulties, determined the equilibrium diagram of manganese and carbon with special care.

## II. Method of experiment and preparation of samples

Thermal analysis, thermal dilatation, microscopic examination, magnetic analysis and X-ray analysis were used for the present study.

Distilled manganese and sugar charcoal were used as alloying materials. Purity of metallic manganese was extremely important in preparing samples. In many investigations hitherto performed, commercial metallic manganese was commonly used, which contained a few per cent of impurities of some kinds. Therefore, metallic manganese purified by the distillation method was used in the present study. The distillation was carried out as follows: about 600 grams of metallic manganese were put in the melting vessel, 127 mm in height, 112 mm in depth, 65 mm in diameter and 6 mm in thickness, made of chemically pure alumina or magnesia powder. The vessel was covered with another vessel of the same size having a small hole in the middle of the bottom to see the interior. Manganese was sublimated on the inner surface of the covered vessel at high temperatures. These vessels were put in a silica tube for evacuation and high frequency induction furnace was used for heating. To prevent manganese from being oxidised, the procedure of filling the silica tube with purified dry hydrogen gas and subsequent evacuating was repeated several times, and the apparatus was then heated to 500 ~ 600°C to take out the final trace of oxidizing gas. When the temperature of distillation was low, impurities and slags at the surface of the melt disturbed the distillation and, accordingly, the efficiency of distillation was lowered. On the

---

(4) R. Vogel and W. Doring, *Archiv. Eisenhüttenw.*, **9** (1935), 247.

contrary, when the temperature was high, metallic and non-metallic impurities also evaporated and, consequently, the purity of distilled manganese became low. Hence, in the present experiment, the distillation of manganese was carried out at 1300~1350°C, and 250~300 grams of manganese with the purity of 99.9 per cent could be obtained in 2.5 hours.

The specimens were prepared from sugar charcoal and distilled manganese, but it was difficult to obtain always a specimen of desired composition by adding carbon directly to manganese. Therefore, several kinds of mother alloys containing about three to four per cent of carbon or of the saturated carbon were first melted in vacuo, and then, manganese alloys containing different amount of carbon were melted with distilled manganese or with mother alloys thus obtained. Magnesia crucibles made of chemically pure magnesia powder in our laboratory were used for melting specimens throughout the experiments.

For thermal analysis, a specially designed vacuum furnace<sup>(5)</sup> of Tammann's type or the ordinary Tammann's furnace with hydrogen gas was used, and for the measurement of magnetic susceptibility, the modified Weiss' method<sup>(6)(7)</sup> was used.

To avoid the oxidation and decarburization of the specimen during the magnetic analysis at high temperatures, the specimen was sealed in transparent silica tube after evacuation. Fig. 1 shows the method of making the specimen holder. The specimen was first placed in the silica tube of the form shown in (a) and then its top end was sealed as shown in (b). In order to avoid the mutual action between the tube and the

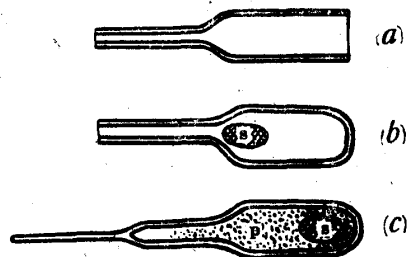


Fig. 1. Example of procedure for making the specimen holder made from transparent silica tube. s specimen, p alumina powder

specimen at high temperatures and to fix the position of the specimen in tube, the space between them was filled with chemically pure alumina powder burned at high temperatures for several hours. The slender end of the tube was connected with a mercury diffusion pump and the tube was evacuated at 400°C for a long time and then sealed as shown in (c). At the slender end a long, slender silica tube, about 3 mm in diameter and about 130 mm in length, was fused to connect the specimen holder with the magnetic apparatus. The specimen holder was about 10 mm in diameter and about 40 mm in length at the portion enclosing the specimen, and about 5 mm in diameter and about 40 mm in length at the adjacent portion. Thus, the care was taken to prevent the tube from bending caused by its weight at high temperatures.

(5) T. Ishiware and M. Isobe, *Nippon Kinzoku Gakkai-si*, **9** (1945), N. 7, 3.

(6) Y. Shimizu. *Sci. Rep., Tohoku Imp. Univ.*, **19** (1930), 411.

(7) M. Isobe, *Sci. Rep., RITU, Tohoku Univ.*, **3** (1951), 78.

III. Results of experiments

Fig.2 shows the equilibrium diagram of manganese and carbon alloy determined in the present study. A brief explanation will be given below.

When carbon is added to manganese, the melting point of the alloy falls first very slowly and a minimum point appears with 1.3 per cent of carbon at 1230°C. Then, gradually rises and finally reaches about 1345°C at 8.6 per cent of carbon.

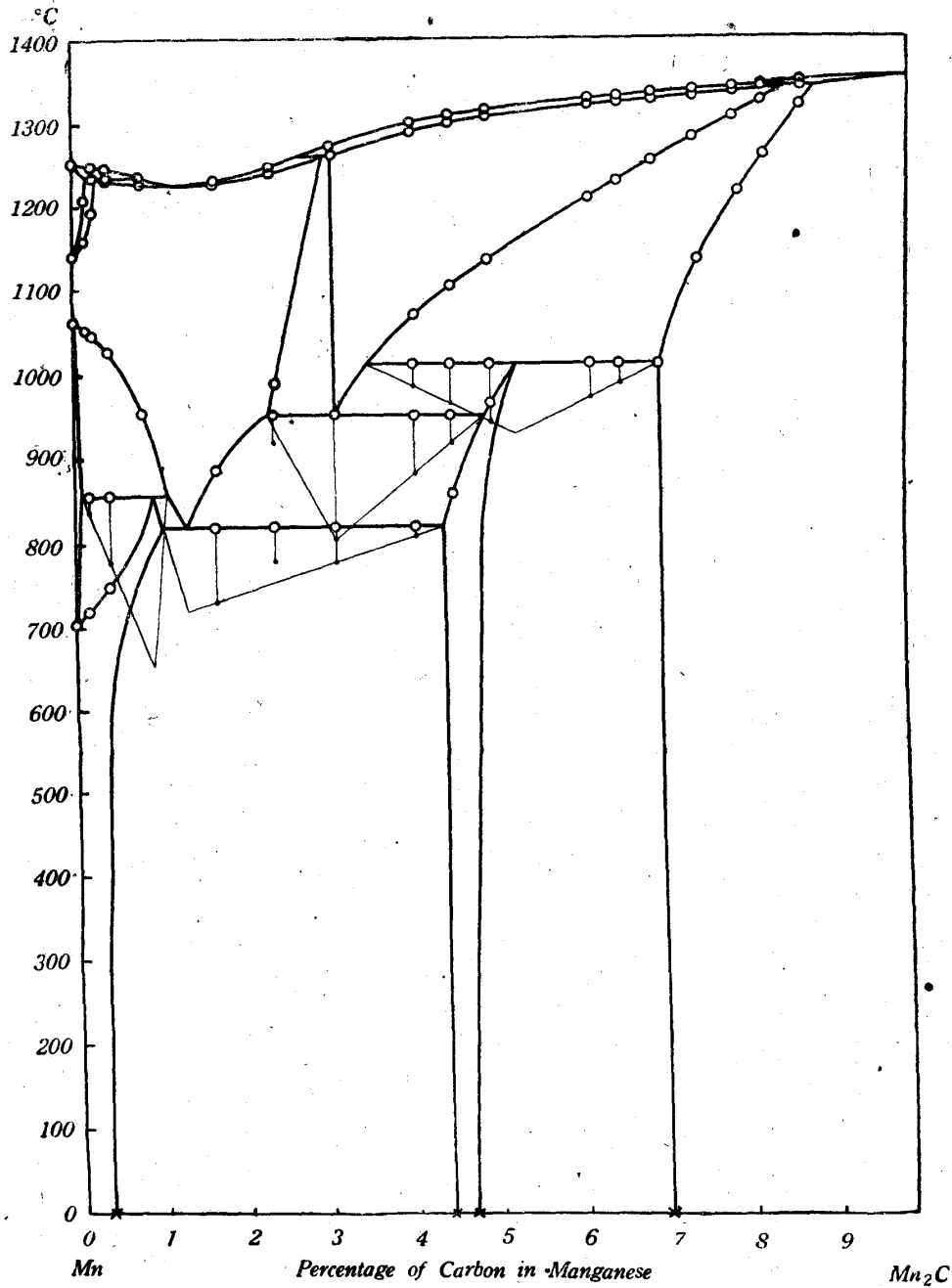


Fig. 2. Equilibrium diagram of manganese and carbon alloy. (by magnetic analysis)

Three kinds of peritectic reactions occur at the time of solidification as follows:

- (1) liquid (0.8%C) +  $\delta$ -manganese solid solution (0.12%C)  $\rightleftharpoons$   $\gamma$ -manganese solid solution (0.25%C) at 1235°C;
- (2) liquid (2.7%C) +  $\beta$ C solid solution (3.05%C)  $\rightleftharpoons$   $\gamma$ -manganese solid solution (2.95%C) at 1260°C;
- (3) liquid (7.5%C) +  $\alpha$ C solid solution (8.75%C)  $\rightleftharpoons$   $\beta$ C solid solution (8.4%C) at 1340°C.

In solid state, pure manganese has four kinds of phases,  $\alpha$ ,  $\beta$ ,  $\gamma$  and  $\delta$ , whose transformation points may be denoted, say, by  $M_1$ ,  $M_2$  and  $M_3$ , respectively. Among these transformations, the  $M_3$  ( $\gamma \rightleftharpoons \delta$ -manganese) point gradually rises with the content of carbon and meets the solidus line, at which the peritectic reaction (1) just mentioned above occurs. The  $M_2$  ( $\beta \rightleftharpoons \gamma$ -manganese) point gradually falls with the content of carbon, while the  $M_1$  ( $\alpha \rightleftharpoons \beta$ -manganese) point gradually rises and the two points finally meet each other at about 857°, at which the following peritectoid reaction occurs:

- (4)  $\gamma$ -manganese solid solution (1.1%C) +  $\beta$ -manganese solid solution (0.05%C)  $\rightleftharpoons$   $\alpha$ -manganese solid solution (0.90%C).

$\gamma$ -manganese solid solution is decomposed, on cooling, into  $\alpha$ -manganese solid solution and  $\gamma$ C solid solution at 820°C as shown in the following eutectoid reaction:

- (5)  $\gamma$ -manganese solid solution (1.3%C)  $\rightleftharpoons$   $\alpha$ -manganese solid solution (1.0%C) +  $\gamma$ C solid solution (4.2%C).

Solubility of carbon in  $\alpha$ -manganese at the eutectoid temperature is 1.0 per cent, but it gradually decreases with the fall of temperature and becomes 0.3 per cent at room temperature.

$\beta$ C solid solution exists in a wide range at high temperatures. Solubility of carbon in this solid solution rapidly decreases with the fall of temperature and, at 1010°C,  $\gamma$ C solid solution is produced from  $\beta$ C and  $\alpha$ C solid solutions in accordance with the following peritectoid reaction:

Table 1. Magnetic susceptibilities of manganese and carbon binary alloys at room temperature.

%C	$\times 10^6$	%C	$\times 10^6$
0.00	10.00	4.00	38.60
0.16	74.75	4.29	83.35
0.20	106.69	4.30	85.35
0.21	114.11	4.43	98.60
0.22	122.15	4.90	117.62
0.80	131.51	6.17	80.00
1.66	106.02	6.45	73.00
2.35	89.32	7.00	53.09
2.54	82.94	7.90	44.00
3.06	64.48		

(6)  $\beta\text{C}$  solid solution (3.4%C) +  $\alpha\text{C}$  solid solution (6.9%C)  $\rightleftharpoons$   $\gamma\text{C}$  solid solution (5.18%C).

$\gamma\text{C}$  solid solution thus produced was fit for the composition of  $\text{Mn}_4\text{C}$  and was newly discovered by the present writer. The existence of  $\gamma\text{C}$  solid solution and its range were determined by means of microscopic examination, X-ray analysis and magnetic analysis. The range of existence at room temperature was comparatively small, such as from 4.3 to 4.6 per cent of carbon, and the detection of the single phase of  $\gamma\text{C}$  solid solution by microscope or by other means was comparatively difficult, as a small amount either of  $\alpha$ -manganese solid solution or of  $\alpha\text{C}$  solid solution usually coexisted with it.

$\beta\text{C}$  solid solution is decomposed into two solid solutions,  $\gamma$ -manganese solid solution and  $\gamma\text{C}$  solid solution at  $950^\circ$  in accordance with the following eutectoid reaction :

(7)  $\beta\text{C}$  solid solution (3.0%C)  $\rightleftharpoons$   $\gamma$ -manganese solid solution (2.0%C) +  $\gamma\text{C}$  solid solution (4.8%C).

$\alpha\text{C}$  solid solution exists in alloys containing more than 6.9 per cent of carbon. It was determined by means of microscopic structure, X-ray analysis and magnetic analysis. The maximum solubility of carbon in manganese attained in the present experiment was 8.6 per cent, which seemed to be the solid solution  $\text{Mn}_2\text{C}$  (9.85% $^\circ\text{C}$ ) with dissolved manganese.

Next, several experimental results from which the above conclusions were drawn, will briefly be described in the following paragraphs.

#### IV. Thermal analysis and thermal dilatation

Some remarkable results of thermal analysis are shown with deltoïd marks in Fig. 3. Among these, the results concerning the solidification of alloys well agreed with those of magnetic analysis as shown in Fig. 2.

The thermal dilatation curves are shown in Fig. 4 (a), (b) and also in Fig. 3 with cross marks. The amounts of transformations, namely, the magnitudes of transitions at isothermal transformations are shown with the triangular figures at the lower parts of the respective temperatures.

Alloys containing from 0.16 to 1.00 per cent of carbon showed a series of isothermal change at  $857^\circ\text{C}$  which corresponded to the following peritectoid reaction,  $\beta$ -manganese solid solution +  $\gamma$ -manganese solid solution  $\rightleftharpoons$   $\alpha$ -manganese solid solution. Alloys containing 1.20 to 3.94 per cent of carbon showed a series of isothermal change at about  $820^\circ\text{C}$ , which fit to the following eutectoid transformation,  $\gamma$ -manganese solid solution  $\rightleftharpoons$   $\alpha$ -manganese solid solution +  $\gamma\text{C}$  solid solution.

Alloys containing 2.37 to 4.43 per cent of carbon showed a series of isothermal change at  $950^\circ\text{C}$ , which fit to the following eutectoid transformation,  $\beta\text{C}$  solid solution  $\rightleftharpoons$   $\gamma$ -manganese solid solution +  $\gamma\text{C}$  solid solution, and alloys containing 3.69 to 6.85 per cent of carbon showed the peritectoid reaction,  $\beta\text{C}$  solid solution

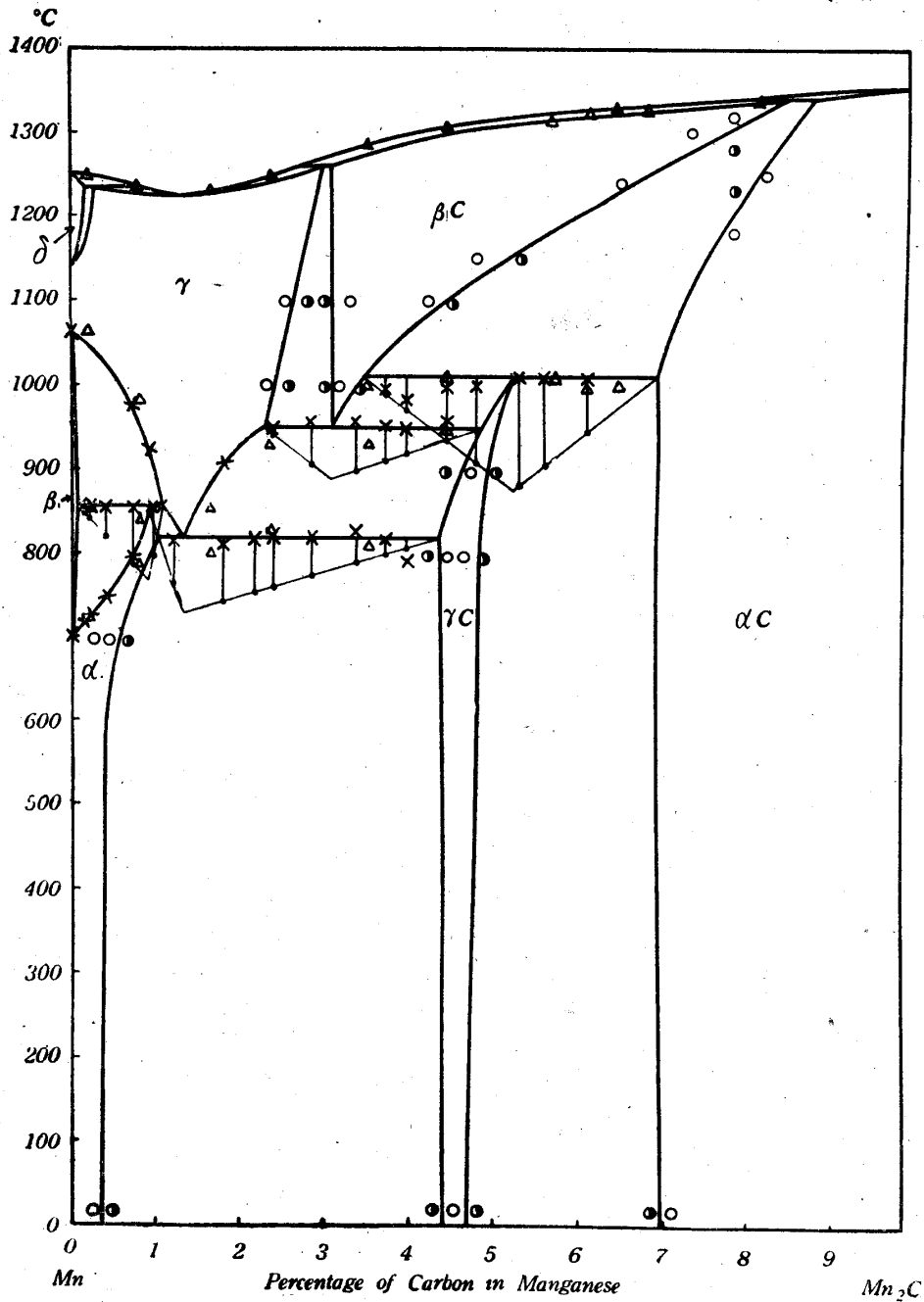


Fig. 3. Equilibrium diagram of manganese and carbon alloy.

- $\Delta$  thermal analysis
- $\times$  thermal dilatation
- $\circ$  microscopic examination, uniform phase
- $\odot$  microscopic examination, two phases

$+\alpha C$  solid solution  $\rightleftharpoons \gamma C$  solid solution, at 1010°C. Accordingly the alloys containing 3.69 to 4.43 per cent of carbon, namely, those of the intermediate compositions between the above two, showed changes in two steps at temperatures above 900°C, which corresponded to the isothermal transformations, namely at 950°C and 1010°C, respectively.



### V. Heat treatment and microscopic structure

Solubility curves were determined by the examination of microscopic structures of samples quenched at various temperatures in ice brine water. In Fig. 3, white and semi-white circles indicate the states of uniform phase and those of two phases, respectively. They are merely examples, the compositions of which were near by the solubility curves.

Next, the microscopic structures of various samples subjected to various thermal treatments were examined and the results were compared with the diagram. Some typical examples will be shown below.

Photo. 1 shows the uniform structure of pure  $\alpha$ -manganese annealed at high temperatures. Photos. 2, 3, 4 and 5 show the annealed structures of alloys containing 1.78, 2.37, 3.36 and 4.6 per cent of carbon, respectively. Samples with low percentage of carbon show large amount of the coloured constituent of  $\alpha$ -manganese solid solution, and that of  $\gamma$ C solid solution with white appearance gradually increases with the content of carbon. Photo. 5 shows the single phase of  $\gamma$ C solid solution. These alloys were all etched with alcoholic solution of two per cent of hydrochloric acid. When the alcoholic solution of nitric acid or picric acid was used as an etchant, the constituents of alloys were inversely coloured, that is,  $\alpha$ -manganese solid solution became colourless, while  $\gamma$ C solid solution was easily coloured.

Photos. 6, 7, 8, 9, 10 and 11

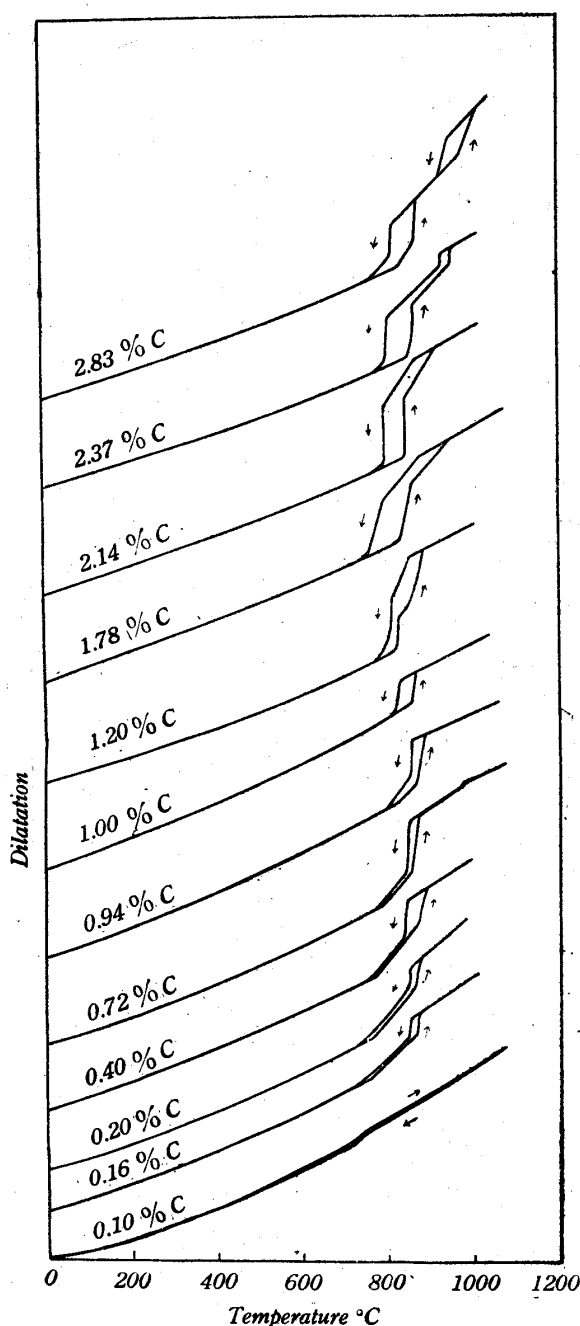


Fig. 4. (a) Thermal dilatation curves of manganese and carbon alloys.

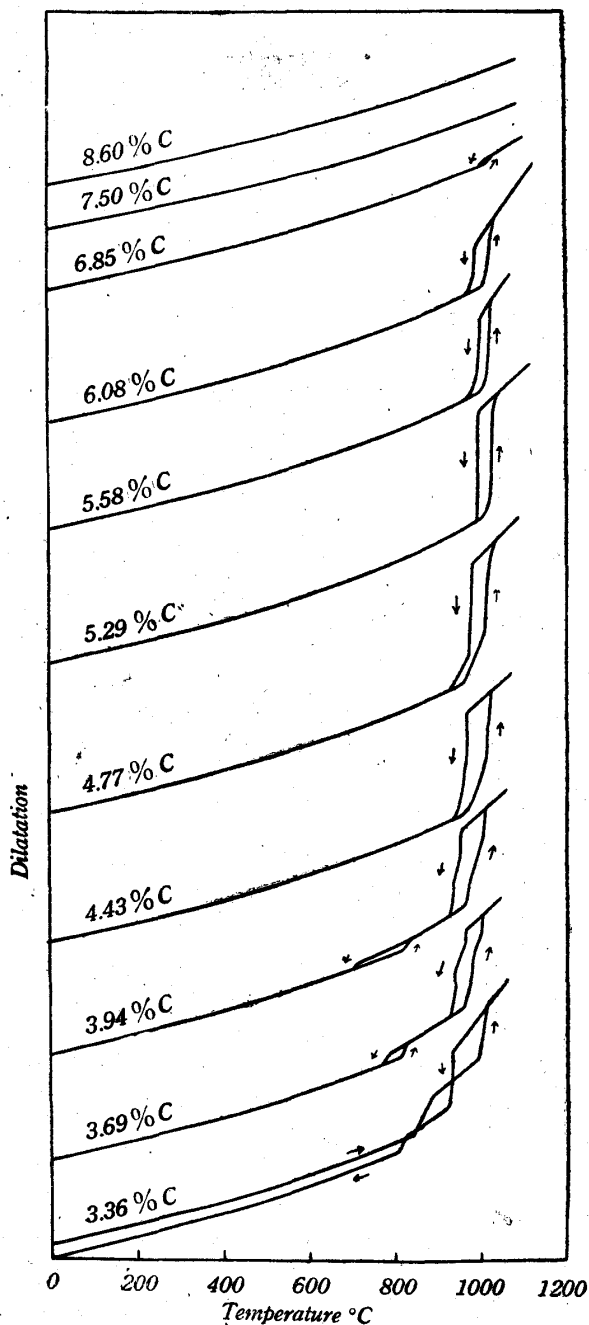


Fig. 4 (b) Thermal dilatation curves of manganese and carbon alloys.

are structures of the alloys containing 4.6, 5.1, 5.55, 6.17, 6.45 and 6.85 per cent of carbon, respectively. After annealing, these alloys were again heated to 1000°C and then cooled at an extremely slow rate to make the reaction,  $\alpha\text{C}$  solid solution +  $\beta\text{C}$  solid solution  $\rightleftharpoons$   $\gamma\text{C}$  solid solution complete. In this case the picral was used as an etchant. Photo. 6 shows the structure of nearly uniform  $\gamma\text{C}$  solid solution. In Photos. 7 to 11, the structures seen white in relief and not easily attacked are all  $\alpha\text{C}$  solid solution in the ground mass of  $\gamma\text{C}$  solid solution, whose amount increase with carbon contents. Photo 11 shows the structure of nearly uniform  $\alpha\text{C}$  solid solution. Photo. 12 shows the structure of annealed  $\alpha\text{C}$  solid solution containing 8.12 per cent of carbon.

Photo. 13 shows the structure of uniform  $\gamma$ -manganese solid solution containing 1.78 per cent of carbon and quenched at 1100°C in ice brine water. Photo. 14 shows the structure of two phases of  $\gamma$ -manganese and  $\beta\text{C}$  solid solution in the alloy containing 2.8 per cent of carbon and quenched at 1100°C in freez-

ing mixture. Photos. 15 and 16 show the structures of alloys of the same composition as the above, being magnified 400 and 1000 times, respectively. The appearance of a part of  $\gamma$ -manganese solid solution is martensitic, and a part of  $\beta\text{C}$  solid solution has the appearance of an assembly of parallels which was not comparatively easily etched. In these samples, the phases stable at high temperatures were not obtained at room temperature by ordinary quenching, because of rapid

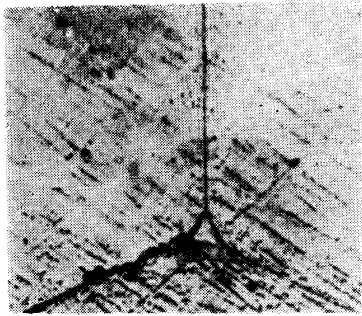


Photo. 1 pure Mn  $\times 400$   
annealed, etched with 2%  
HCl alcoholic solution.

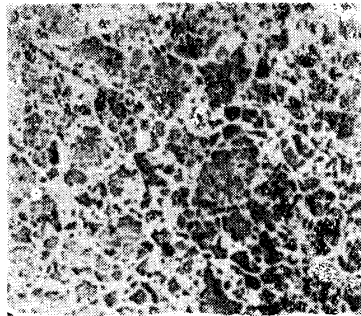


Photo. 2 1.78% C  $\times 100$   
annealed, etched with 2%  
HCl alcoholic solution.

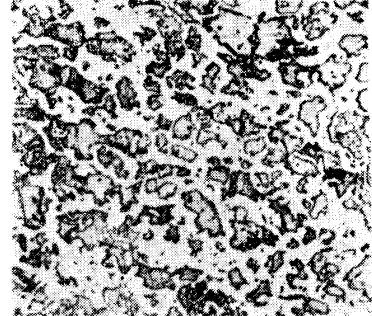


Photo. 3 2.37% C  $\times 100$   
annealed, etched with 2%  
HCl alcoholic solution.

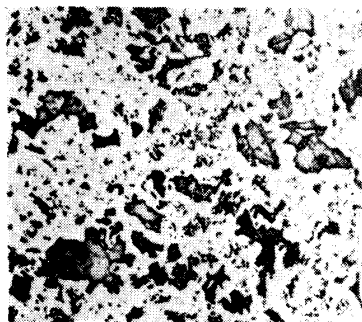


Photo. 4 3.36% C  $\times 100$   
annealed, etched with 2%  
HCl alcoholic solution.

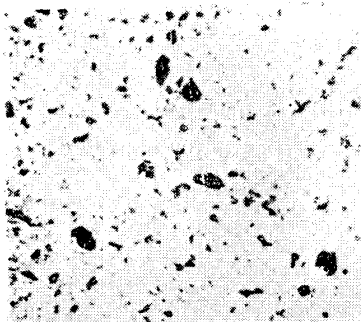


Photo. 5 4.6% C  $\times 100$   
annealed, etched with 2%  
HCl alcoholic solution.

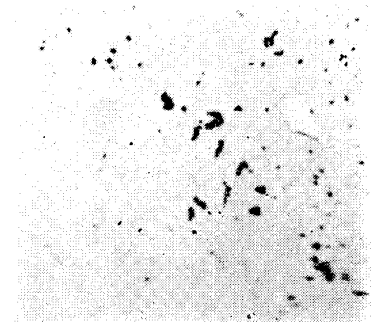


Photo. 6 4.6% C  $\times 400$   
annealed, etched with  
picral.

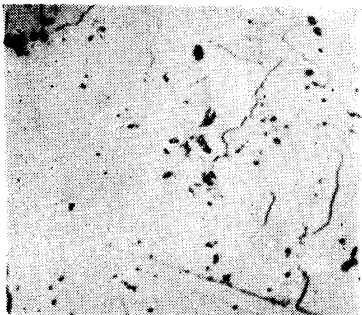


Photo. 7 5.1% C  $\times 400$   
annealed, etched with  
picral.

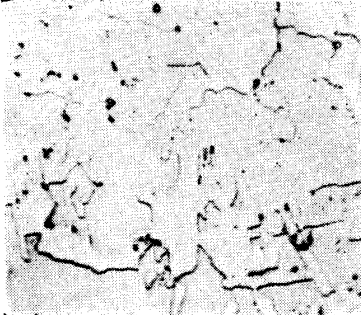


Photo. 8 5.55% C  $\times 400$   
annealed, etched with  
picral.

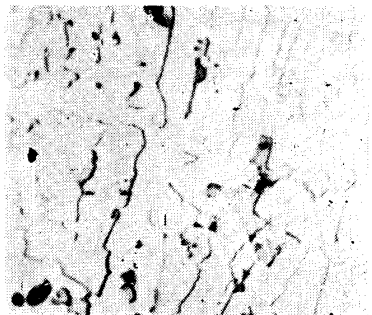


Photo. 9 6.17% C  $\times 400$   
annealed, etched with  
picral.

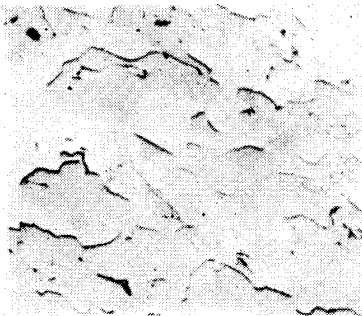


Photo. 10 6.45% C  $\times 400$   
annealed, etched with  
picral.

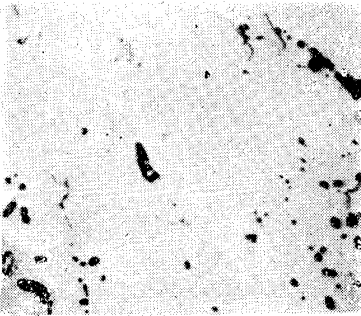


Photo. 11 6.85% C  $\times 400$   
annealed, etched with  
picral.



Photo. 12 8.12% C  $\times 400$   
annealed, etched with  
picral.

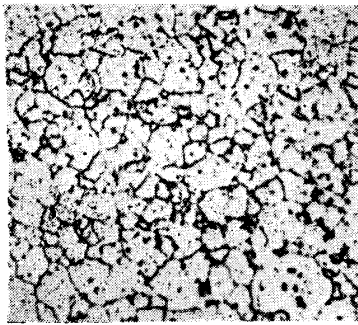


Photo. 13 1.78% C  $\times 100$   
quenched from 1100°C  
in ice brine water.

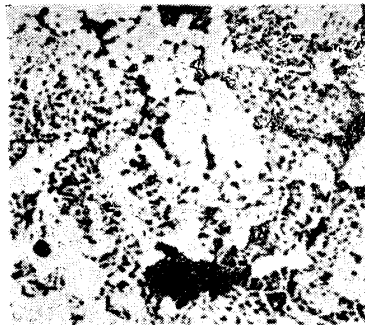


Photo. 14 2.8% C  $\times 100$   
quenched from 1100°C  
in ice brine water.



Photo. 15 2.8% C  $\times 400$   
quenched from 1100°C  
in ice brine water.



Photo. 16 2.8% C  $\times 1000$   
quenched from 1100°C  
in ice brine water.

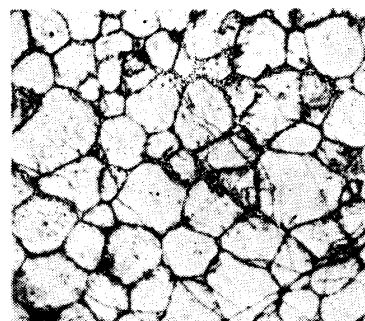


Photo. 17 3.69% C  $\times 100$   
quenched from 1100°C  
in ice brine water.

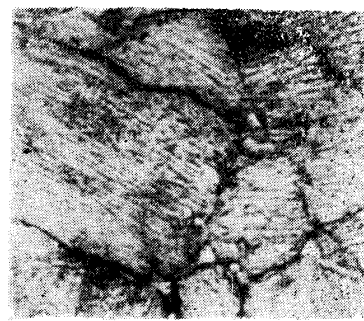


Photo. 18 3.53% C  $\times 400$   
quenched from 1100°C  
in ice brine water.



Photo. 19 7.29% C  $\times 150$   
quenched from 1300°C  
in ice brine water.

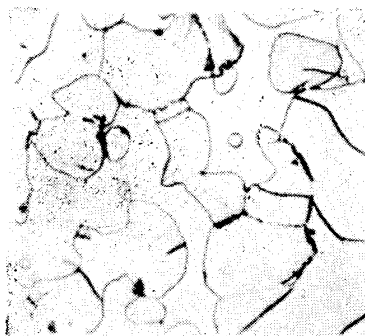


Photo. 20 5.21% C  $\times 400$   
quenched from 1100°C  
in ice brine water.

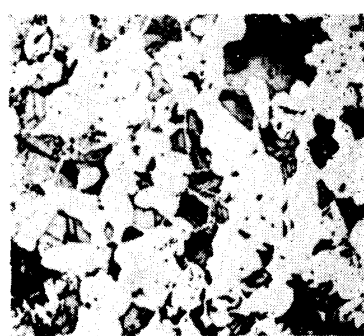


Photo. 21 7.5% C  $\times 100$   
quenched from 1230°C  
in ice brine water.



Photo. 22 8.12% C  $\times 400$   
quenched from 1250°C  
in ice brine water.

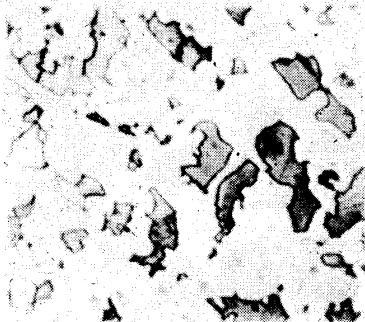


Photo. 23 4.43% C  $\times 400$   
quenched from 1000°C  
in ice brine water.

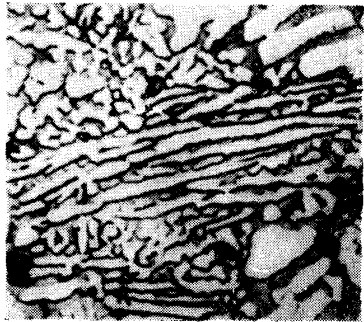


Photo. 24 3.1% C  $\times 100$   
quenched from 900°C  
in ice brine water.

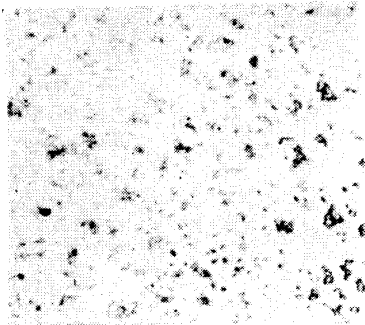


Photo. 25 4.21% C  $\times 100$ ,  
quenched from 900°C  
in ice brine water.

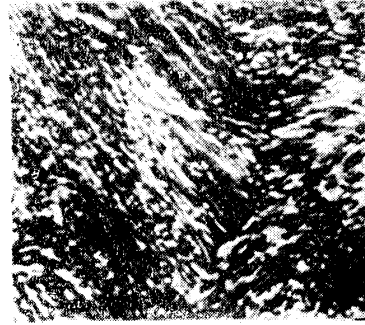


Photo. 26 1.27% C  $\times 1000$   
annealed.

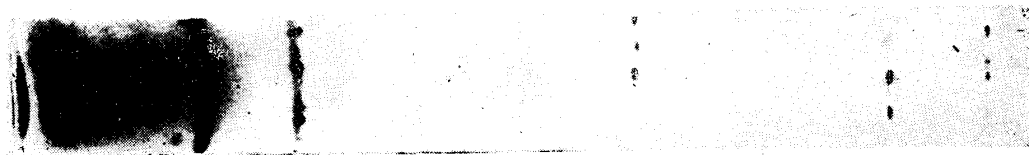


Photo. 27 1.78% C, quenched from 1100°C, in ice brine water.

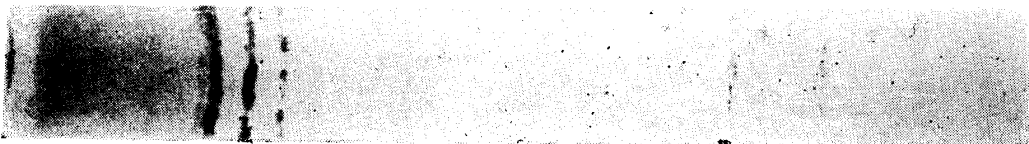


Photo. 28 pure manganese, quenched from 900°C in ice brine water.

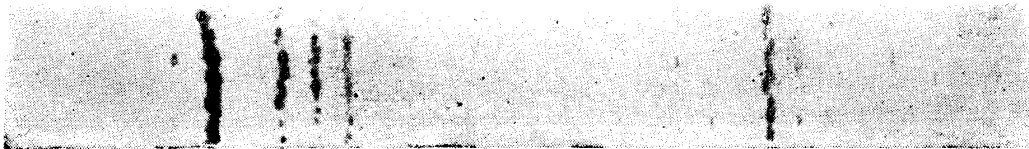


Photo. 29 pure manganese, annealed.



Photo. 30 7.82% C, annealed.

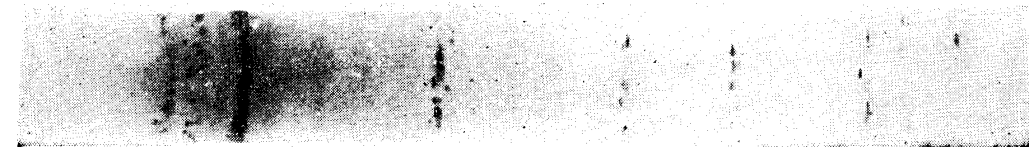


Photo. 31 4.21% C, quenched from 1100°C in ice brine water.

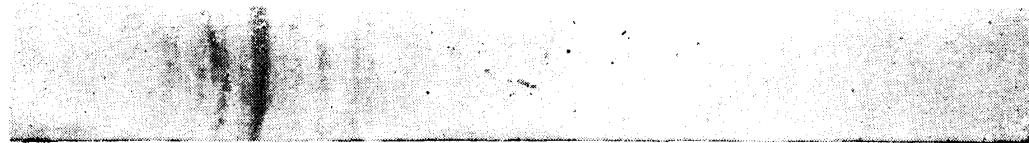


Photo. 32 4.60% C, quenched from 800°C in ice brine water.

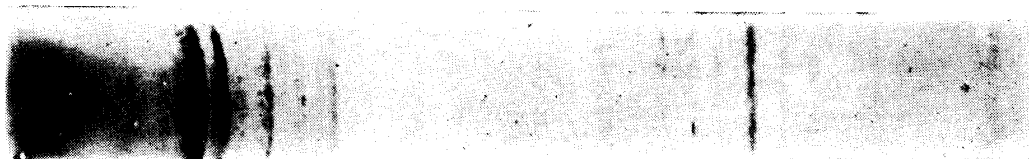


Photo. 33 2.55%C, annealed.

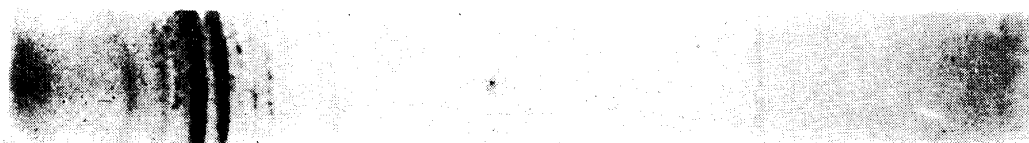


Photo. 34 3.13%C, annealed.

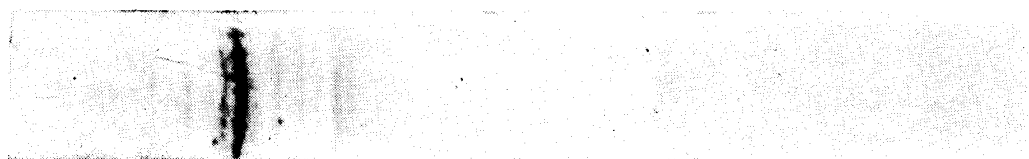


Photo. 35 6.07%C, annealed.

transformation rates; hence, their microstructures were almost the same, when they were quenched. Photo. 17 shows the uniform  $\beta$ C solid solution containing 3.69 per cent of carbon and quenched at 1100°C in freezing mixture. Photo. 18 shows the uniform  $\beta$ C solid solution containing 3.53 per cent of carbon, quenched at 1100° in freezing mixture and magnified 400 times, in which many parallels are seen. Photo. 19 shows the uniform  $\beta$ C solid solution containing 7.29 per cent of carbon and quenched at 1300°C in ice brine water, in which the change during cooling is scarcely observable. Photos. 20 and 21 show the structures of alloys containing 5.21 and 7.5 per cent of carbon and quenched at 1100°C and 1230°C, respectively. They consist of two phases of  $\beta$ C and  $\alpha$ C solid solutions, the coloured part being  $\beta$ C solid solution and the white part  $\alpha$ C solid solution. Photo. 22 shows nearly uniform  $\alpha$ C solid solution containing 8.12 per cent of carbon and quenched at 1250°C in ice brine water, in which black part was caused by the defect in preparing specimen.

Photo. 23 shows the structure of an alloy containing 4.43 per cent of carbon and quenched at 1000°C in ice brine water, black part being  $\beta$ C solid solution and white part  $\gamma$ C solid solution. Photo. 25 shows the structure of an alloy containing 4.21 per cent of carbon and quenched at 900°C in ice brine water, which consists of two phases of  $\gamma$ -manganese and  $\gamma$ C solid solution, and the most of structures are white  $\gamma$ C solid solution mixed with a small amount of  $\gamma$ -manganese solid solution.

Photo. 24 shows the eutectoid structure containing 3.1 per cent of carbon and quenched at the temperature just below that of the following reaction:  $\beta$ C solid solution  $\rightleftharpoons$   $\gamma$ -manganese solid solution +  $\gamma$ C solid solution. Hence, it consisted of two phases of  $\gamma$ -manganese and  $\gamma$ C solid solution.

Photo. 26 shows the pearlitic structure of alloy containing 1.27 per cent of carbon and cooled slowly after heated for 100 hours at 800°C, i. e., just below 820°, at which the following eutectoid reaction took place:  $\gamma$ -manganese solid solution  $\rightleftharpoons$   $\alpha$ -manganese solid solution +  $\gamma$ C solid solution.

## VI. X-ray analysis

X-ray analysis was made by the methods of Zeemann and of Debye-Scherrer with a large number of heat treated samples. Iron anti-cathode was used and the diameter of camera was 70 mm. Some typical examples will be shown below.

Photo. 27 shows the  $\gamma$ -manganese solid solution containing 1.78 per cent of carbon and quenched at 1100°C in freezing mixture. Photos. 28 and 29 show the  $\beta$ -manganese and  $\alpha$ -manganese, respectively, both being quenched at 900°C and then annealed.

Photo. 30 shows the  $\alpha$ C solid solution containing 7.82 per cent of carbon and annealed. Photo. 31 shows the  $\beta$ C solid solution containing 4.21 per cent of carbon and quenched at 1100°C. Photo. 32 shows the  $\gamma$ C solid solution containing 4.60 per cent of carbon and quenched at 800°C. By comparing these three photographs with one another, it will be seen that the  $\alpha$ C,  $\beta$ C and  $\gamma$ C solid solutions are mutually independent phases.

Photos. 33 and 34 are those of alloys containing 2.55 and 3.13 per cent of carbon, respectively, and slowly cooled after prolonged heating at temperature below 800°C. Both are the mixtures of  $\alpha$ -manganese and  $\gamma$ C solid solution, the lines of  $\alpha$ -manganese solid solution being strong in the former, whereas those of  $\gamma$ C solid solution being clear in the latter. Photo. 35 shows the mixture of the two phases of  $\gamma$ C and  $\alpha$ C solid solutions, containing 6.07 per cent of carbon, annealed and slowly cooled in 100 hours from 1000° to 700°C.

## VII. Determination of solubility limit by means of magnetic method

There is a certain relation between the magnetic susceptibility and the composition of a binary alloy. The present writer reported<sup>(8)</sup> the results of measurements on many binary alloy series. In the present case, the solubility limits at room temperature were also determined by the same method as the former and the results are shown in Table I.

Fig. 5 shows the relationship between the magnetic susceptibility and the composition of alloy at room temperature. As seen in Fig. 5, the magnetic susceptibility of an alloy first increases rapidly with a small amount of carbon, reaching  $\chi=146 \times 10^{-6}$  at 0.3 per cent of carbon and then straightly decreases to  $\chi=32 \times 10^{-6}$  at 4.3 per cent of carbon, and again increases to  $\chi=127 \times 10^{-6}$  at 4.6

(8) H. Endo and M. Isobe, *Kinzoku no Kenkyu*, **3** (1926), 492, 505; **4** (1927), 150.

per cent of carbon. With further increase of carbon, it decreases straightly until about 7 per cent of carbon and then decreased slowly.

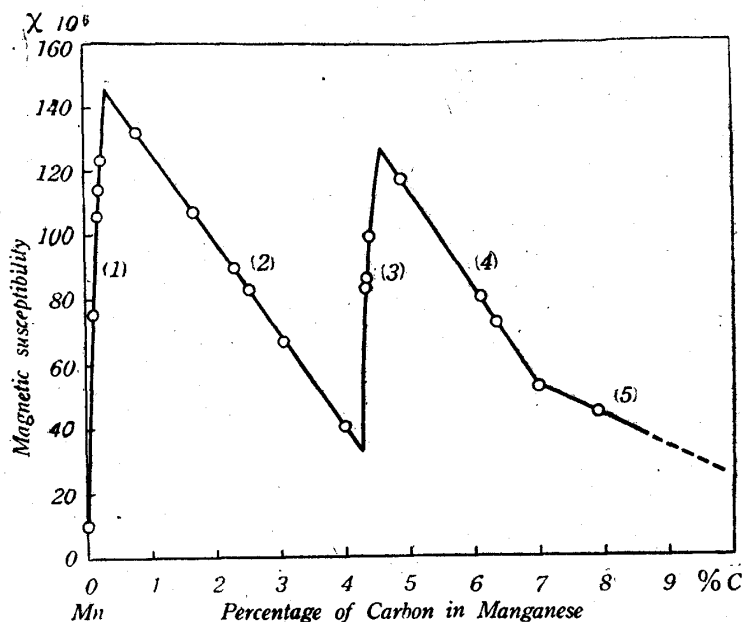


Fig. 5. Relation between magnetic susceptibility and composition at room temperature.

- (1)  $\alpha$ -manganese solid solution
- (2)  $\alpha$ -manganese and  $\gamma$ C solid solution
- (3)  $\alpha$ C solid solution
- (4)  $\gamma$ C and  $\alpha$ C solid solution
- (5)  $\alpha$ C solid solution

straightly showing the existence of a mixture in this region. Indeed, there was a mixture of  $\alpha$ -manganese and  $\gamma$ C solid solution. The rapid and winding increase of susceptibility at the region from 4.3 to 4.6 per cent of carbon shows that the alloys in this range are a single solid solution which corresponds to  $\gamma$ C solid solution newly discovered by the present writer as already mentioned.

In alloys containing more than 4.6 per cent of carbon, the susceptibility again decreases straightly to 7.0 per cent of carbon, showing the existence of a mixture of  $\gamma$ C and  $\alpha$ C solid solution.

Above 7.0 per cent of carbon, the change in susceptibility was small, which agreed well with the results that the alloys with higher carbon content were uniform  $\alpha$ C solid solution.

### VIII. Magnetic analysis at high temperatures

Magnetic analysis was most effective in the determination of the phase boundary, the results of which are shown in Figs. 6 (a) and 6 (b). For convenience of explanation, notations annexed to the curves denoting phases and non-variant reactions will first be summarized.

Comparing this result with the diagram of Fig. 2, the rapid and winding increase in magnetic susceptibility with a small amount of carbon may be seen, which shows the existence of  $\alpha$ -manganese solid solution in this region. Hence, it may be said that the solubility of carbon in manganese at room temperature will be 0.3 per cent. In alloys containing 0.3 to 4.3 per cent of carbon the susceptibility changed



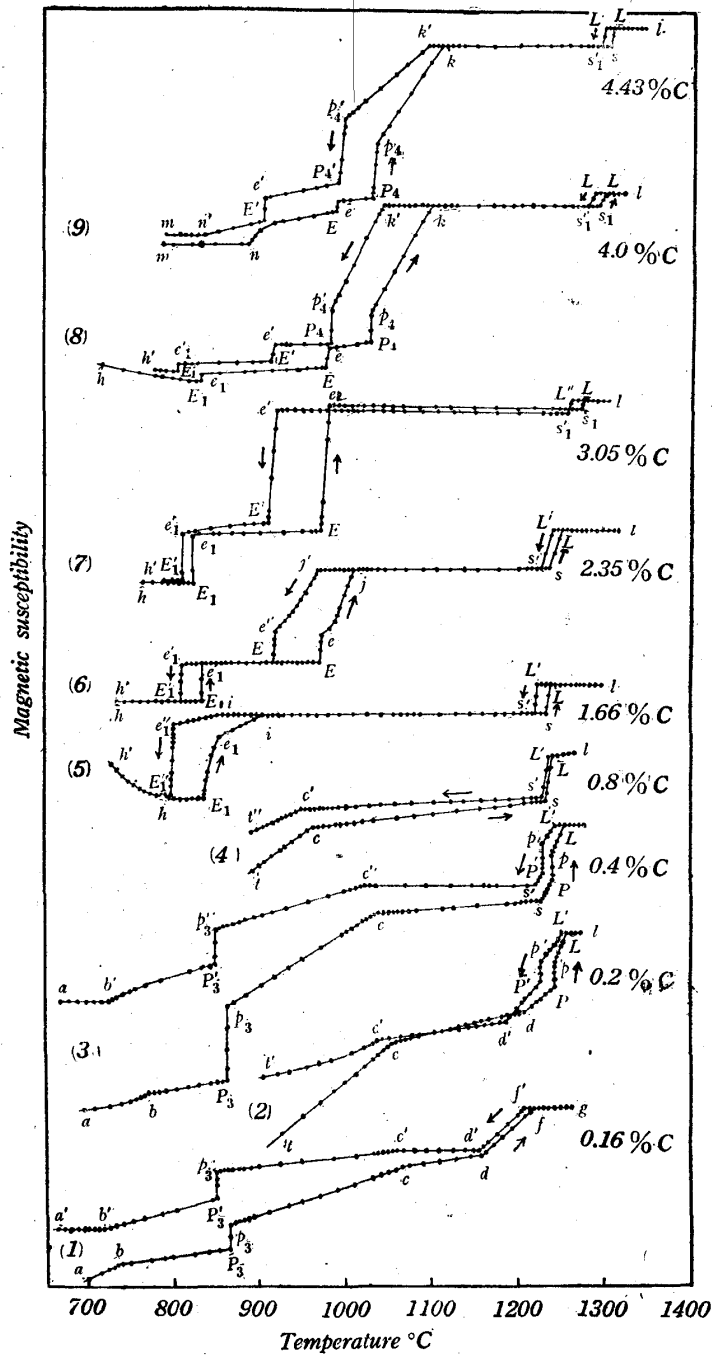


Fig. 6 (a) Magnetic analysis curves of manganese and carbon alloys.

- ab  $\alpha$ -manganese solid solution
- bP<sub>3</sub>  $\alpha$  and  $\beta$ -manganese solid solutions
- P<sub>3</sub>P<sub>3</sub> peritectoid reacton,  $\beta$ -manganese solid solution +  $\gamma$ -manganese solid solution  $\rightleftharpoons$   $\alpha$ -manganese solid solution, at 857°C
- p<sub>3</sub>c, tc  $\beta$  and  $\gamma$ -manganese solid solutions
- cd, cs, is, js  $\gamma$ -manganese solid solution

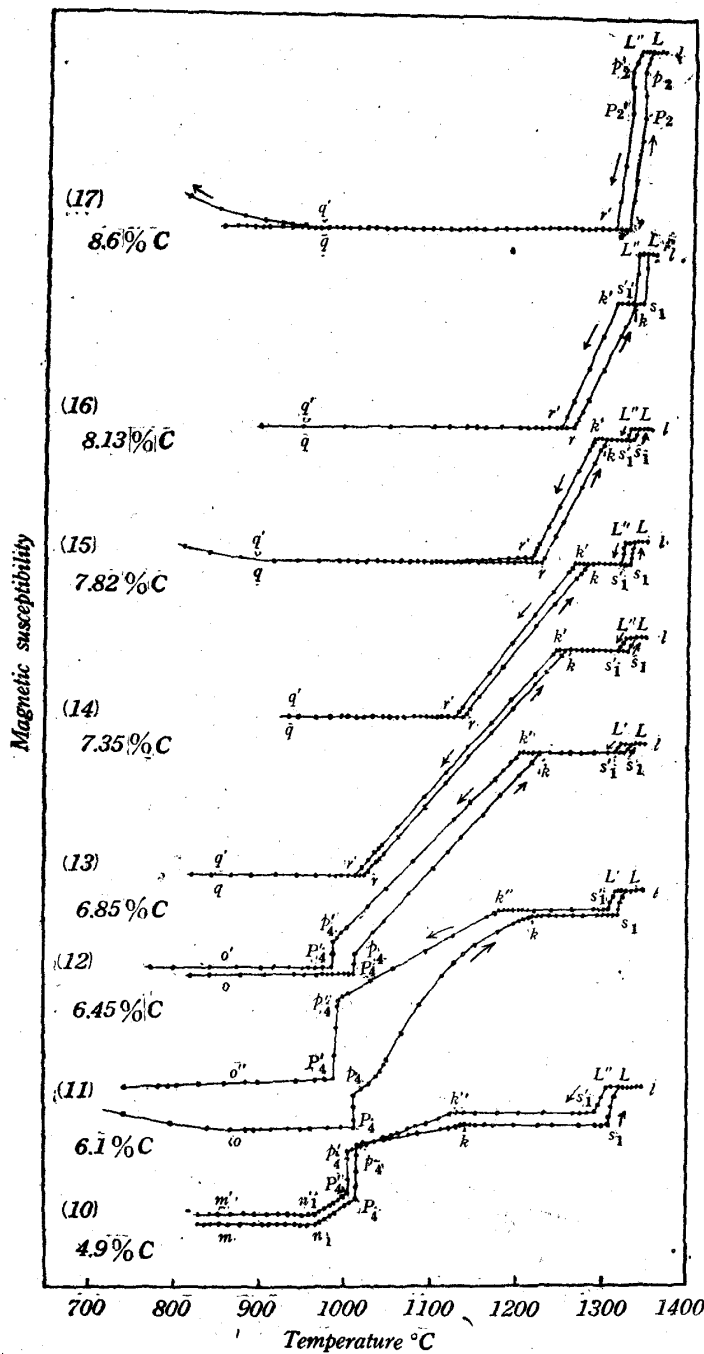


Fig. 6 (b) Magnetic analysis curves of manganese and carbon alloys.

- df, dP      γ and δ-manganese solid solutions
- fg          δ-manganese solid solution
- Pp          peritectic reaction, liquid + δ-manganese solid solution ⇌ γ-manganese solid solution, at 1235°C
- pL          liquid + δ-manganese solid solution
- L1          liquid

sP, sL	liquid + $\gamma$ -manganese solid solution
hE <sub>1</sub>	$\alpha$ -manganese solid solution + $\gamma$ C solid solution
E <sub>1</sub> e <sub>1</sub>	eutectoid reaction, $\gamma$ -manganese solid solution $\rightleftharpoons$ $\alpha$ -manganese solid solution + $\gamma$ C solid solution, at 820°C
e <sub>1</sub> i, e <sub>1</sub> E, nE	$\gamma$ -manganese solid solution + $\gamma$ C solid solution
Ee	eutectoid reaction, $\beta$ C solid solution $\rightleftharpoons$ $\gamma$ -manganese solid solution + $\gamma$ C solid solution, at 950°C
ej	$\gamma$ -manganese solid solution + $\beta$ C solid solution
s <sub>1</sub> L	liquid + $\beta$ C solid solution
es <sub>1</sub> , ks <sub>1</sub>	$\beta$ C solid solution
P <sub>4</sub> p <sub>4</sub>	peritectoid reaction, $\beta$ C solid solution + $\alpha$ C solid solution $\rightleftharpoons$ $\gamma$ C solid solution, at 1010°C
p <sub>4</sub> k, rk, rP <sub>2</sub>	$\alpha$ C solid solution + $\beta$ C solid solution
mn, mn <sub>1</sub>	$\gamma$ C solid solution
eP <sub>4</sub> , n <sub>1</sub> P <sub>4</sub>	$\beta$ C solid solution + $\gamma$ C solid solution
oP <sub>4</sub>	$\gamma$ C solid solution + $\alpha$ C solid solution
qr	$\alpha$ C solid solution
P <sub>2</sub> p <sub>2</sub>	peritectic reaction, liquid + $\alpha$ C solid solution $\rightleftharpoons$ $\beta$ C solid solution, at 1340°C
p <sub>2</sub> L	liquid + $\alpha$ C solid solution

Next, brief interpretations of the curves will be given below.

Curve (1) shows the result of the alloy containing 0.16 per cent of carbon. The segment ab is the region of  $\alpha$ -manganese solid solution, which is followed at the point b by a gradual increase in amount of  $\beta$ -manganese solid solution. The isothermal change denoted by P<sub>3</sub>p<sub>3</sub> at 857°C is the peritectoid reaction, after which the alloy is composed of two phases of  $\beta$  and  $\gamma$ -manganese solid solutions, and, with further rises in temperature, the amount of  $\beta$ -manganese solid solution gradually decreases, and finally, the alloy becomes a single phase of uniform  $\gamma$ -manganese solid solution at the point c. The magnetic susceptibility of  $\gamma$ -manganese solid solution does not change further on continued heating. The change of  $\gamma$ -manganese solid solution into  $\delta$  begins at the point d and ends at the point f, the two-phase region being df. As shown by the segment fg, the magnetic susceptibility of  $\delta$ -manganese solid solution does not change further on heating. On cooling, the susceptibility changed in the order reverse to the above as shown by the curve gf'd'c'p<sub>3</sub>'P<sub>3</sub>'b'a'.

Curve (2) shows the magnetic property of the alloy containing 0.2 per cent of carbon at high temperatures. The segment tc is two-phase region of  $\beta$  and  $\gamma$ -manganese solid solutions, and the change from  $\gamma$ -manganese solid solution to  $\delta$  begins at the point d, the segment df being two-phase region of  $\gamma$  and  $\delta$ -manganese solid solutions. The isothermal change Pp at 1235°C is the peritectic reaction. The alloy in the segment PL is composed of  $\delta$ -manganese solid solution and liquid.

At the temperature above the point L the alloy melts.

As it will be seen from curves (1) and (2),  $M_1$  transformation of manganese gradually rises with carbon content. Peritectoid reaction is also clearly seen in it and the magnitude of this transformation on curve (2) is larger than that on the curve (1).  $M_2$  transformation of manganese is gradually falls with carbon content, which can be confirmed by comparing the point c on the respective curves (1), (2), (3) and (4). The rise in  $M_3$  transformation of manganese with carbon content is clearly seen from the point d or the segments df and dp on curves (1) and (2), respectively.

The change in magnetic susceptibility in the curves (5), (6), (7) and (8) are small up to the transformation temperature, but at 820°C a sudden increase in susceptibility is seen in every curve, which indicates eutectoid reaction. In the case of curve (5), this change is larger than those in other curves and, with further rise in temperature, the solubility of  $\gamma$ C in  $\gamma$ -manganese solid solution increases up to the point i and then the alloy consists of a uniform phase of  $\gamma$ -manganese solid solution as shown by the horizontal segment is. In the curves (6), (7) and (8), another eutectoid reaction takes place at 950°C as shown by the segment Ee, the magnitude in the curve (7) being the largest. In the alloys containing more than 4.0 per cent of carbon, another sudden increase in susceptibility denoted by  $P_4p_4$  appears at 1010°C, which is a peritectoid reaction, while the eutectoid reaction at 820°C disappears. Thus, the alloys containing 3.05 to 4.43 per cent of carbon show three isothermal transformations as shown in the curves (7), (8) and (9). The magnitude of the eutectoid reaction at 950°C becomes small with the increase of carbon content and vanishes from observation with the alloys containing more than 4.9 per cent of carbon.

The change in susceptibility due to the peritectoid reaction at 1010°C denoted by the segment  $P_4p_4$  is the largest in the alloy of the curve (10) among those shown in the curve (8)~(12), and the peritectic reaction becomes no longer observable in the curve (13).

The solubility of  $\alpha$ C solid solution in  $\beta$ C solid solution is shown by the point k on the curves (8)~(16), and the solubility line gradually rises as the content of carbon increases and finally meets the solidus line, at which the peritectic reaction takes place. In the case of the curve (17) the segment  $P_2p_2$  is the peritectic reaction at 1340°C. The behavior of the curves (14), (15) and (16) are similar to that of the curve (14), although the two-phase region of  $\alpha$ C and  $\beta$ C solid solutions is gradually transferred to higher temperature region. The amount of susceptibility of  $\alpha$ C solid solution does not change appreciably with temperature.

The white small circles on the respective curves in Fig. 2 were plotted from the above results, and it will be seen that the several relationships in the diagram were well confirmed by these results of the magnetic analyses and that they also coincided well with those in Fig. 3, which shows the summarized result of thermal dilatation,

thermal analysis and microscopic examination.

### IX. Discussion

As already said, among many studies of the equilibrium diagram of manganese and carbon binary alloy, the result of R. Vogel and E. Doring<sup>(4)</sup> was, in some respects, coincident with the present research and is, therefore, referred to in the following discussion.

#### (1) Solidification

In the study by R. Vogel and W. Doring, commercial manganese was used, the melting point of which was 1230°C against 1252°C in the present research. And, as they did not recognize  $M_3$  ( $\gamma\text{Mn} \rightleftharpoons \delta\text{Mn}$ ) transformation in pure manganese, the region of  $\delta$ -manganese solid solution and the peritectic reaction, liquid +  $\delta$ -manganese solid solution  $\rightleftharpoons$   $\gamma$ -manganese solid solution, were not given in their diagram. As shown in Fig. 2, the alloy containing 1.25 per cent of carbon showed a minimum on liquidus line at about 1225°C. In the case of R. Vogel and W. Doring, the minimum on liquidus appeared at about 1160°C with the composition of nearly 3.5 per cent of carbon. According to other reports, a maximum appeared on liquidus at the middle part of the diagram. This is, however, very improbable from the results of R. Vogel and E. Doring or from the present result. As will be seen clearly in the next report on the study of iron-manganese-carbon ternary alloy diagram by present writer, the minimum point at 1.25 per cent of carbon in Fig. 2 was gradually transferred to the high carbon side in the case in which iron was added to the manganese and carbon alloys. Accordingly, the minimum with higher carbon content in the diagram by R. Vogel and W. Doring might be caused by impurities in metallic manganese used by them. Further, they reported the existence of manganese carbide  $\text{Mn}_3\text{C}$  with melting point 1245°C, but in the present experiment such a carbide was not observable.

#### (2) $\alpha$ , $\beta$ and $\gamma$ -manganese solid solutions

As to the regions of existence and the forms of boundary curves of these three phases, the present results differed from those of Vogel and Doring in detailed parts, but the general tendencies of the transformation and the mode of the reaction between phases coincided well with one another. A remarkably different point was that the temperature of  $M_1$  ( $\alpha\text{Mn} \rightleftharpoons \beta\text{Mn}$ ) was 702°C in the present study against 740°C in the case of R. Vogel and W. Doring. This might, perhaps, be attributed to the difference in the purity of manganese. When iron or carbon was added to pure manganese as impurity, the  $M_1$  transformation point was actually raised. The transformation temperature of  $M_2$  ( $\beta\text{Mn} \rightleftharpoons \gamma\text{Mn}$ ) was 1065°C in the present case against 1140°C in the case of R. Vogel and W. Doring. This difference might also be attributed to the impurity in manganese or to the confusion of  $M_2$  ( $\beta\text{Mn} \rightleftharpoons \gamma\text{Mn}$ ) transformation with  $M_3$  ( $\gamma\text{Mn} \rightleftharpoons \delta\text{Mn}$ , 1138°C).

According to the measurements of magnetic susceptibility, solubility of carbon

in  $\alpha$ -manganese solid solution was about 0.3 per cent at room temperature against about 1 per cent in the case of R. Vogel and W. Doring.

(3)  $\alpha$ C,  $\beta$ C and  $\gamma$ C solid solution

As above described, R. Vogel and W. Doring reported the existence of manganese carbide  $Mn_3C$  with about 6.8 per cent of carbon, which is very similar to the iron carbide  $Fe_3C$ . According to the microscopic examination, X-ray analysis and magnetic analysis, the alloy containing more than 7.0 per cent of carbon clearly showed the structure of  $\alpha$ C solid solution and the composition corresponding to  $Mn_3C$  was merely the phase boundary of  $\alpha$ C solid solution at lower carbon side. In the present experiment, the attainable maximum total carbon in manganese was 8.6 per cent and the properties of alloys containing more carbon than this was not clear, and the  $\alpha$ C solid solution was believed to be the solid solution of the carbide  $Mn_2C$  with dissolved manganese.

The range of existence of the  $\beta$ C solid solution containing 3.05 to 8.40 per cent of carbon and that of the  $\beta$ - $Mn_3C$  solid solution by R. Vogel and W. Doring almost coincided with each other at high temperatures, but the lower parts of phase boundaries were considerably different. That is, R. Vogel and W. Doring believed the existence of the allotropic change of  $Mn_3C$  ( $\alpha$ - $Mn_3C \rightleftharpoons \beta$ - $Mn_3C$ ) at 1050°C and, consequently, the above-mentioned phase boundary was divided by the  $\alpha$ - $\beta$  transformation line (at 1050°C with the composition of  $Mn_3C$  and at 920°C with the composition of about 3.5 per cent of carbon). As often stated, the carbide  $Mn_3C$  was not observable in the present case; hence, the said transformation was, probably, confused with the peritectic reaction.

$\gamma$ C solid solution was produced by the peritectoid reaction of  $\beta$ C and  $\alpha$ C solid solutions at 1010°C and its composition corresponded to  $Mn_4C$ . The formation of  $\gamma$ C solid solution was confirmed by the microscopic examination, X-ray analysis and magnetic analysis.  $\beta$ C solid solution was decomposed into two solid solutions,  $\gamma$ -manganese solid solution and  $\gamma$ C solid solution, by the eutectoid reaction at 950°C, which R. Vogel and W. Doring considered to be the following eutectoid reaction at 920°C:  $\beta$ - $Mn_3C$  solid solution  $\rightleftharpoons$   $\gamma$ -manganese solid solution +  $\alpha$ - $Mn_3C$  solid solution. This error might be due to some circumstance under which they were not able to observe  $\gamma$ C solid solution.

Against the decomposition of  $\gamma$ -manganese into  $\alpha$ -manganese and  $\gamma$ C solid solution at 820°C, R. Vogel and W. Doring stated the existence of the following eutectoid reaction at about 740°C:  $\gamma$ -manganese solid solution  $\rightleftharpoons$   $\alpha$ -manganese solid solution +  $\alpha$ - $Mn_3C$  solid solution. This might also be derived by neglecting the existence of  $\gamma$ C solid solution. Indeed, in their diagram, the above eutectoid line ended at 4.0 per cent of carbon, namely, in the neighbourhood of the boundary (4.3 per cent of carbon) of  $\gamma$ C solid solution. The eutectoid reaction was not actually observable in alloys containing more carbon than this, whereas the eutectoid line was drawn by them to the composition corresponding to  $Mn_3C$ . Owing to the

extreme difficulty in the microscopic confirmation of  $\gamma$ C solid solution, a very long annealing at the temperature just below the peritectoid point, say, for 100 hours, was necessary to obtain the uniform phase of  $\gamma$ C solid solution. In the experiments of Vogel and Doring, such a special care might not be taken, and, consequently, the observations were probably misled.

### Summary

The present investigation may be summarized as follows:

(1) Manganese and carbon binary alloys were made by using distilled manganese and sugar charcoal.

(2) Thermal analysis, thermal dilatation, X-ray analysis, microscopic examination and magnetic analysis were used in studying the alloys.

(3) Seven kinds of solid solutions,  $\alpha$ -manganese,  $\beta$ -manganese,  $\gamma$ -manganese,  $\delta$ -manganese,  $\alpha$ C,  $\beta$ C and  $\gamma$ C solid solutions were observed.

(4) In this alloy system, there were three kinds of peritectic reactions on solidification.

(5) In the solid state, two kinds of peritectoid reactions and two kinds of eutectoid reactions occurred.

(6) Solubility of carbon in  $\alpha$ -manganese was 0.3 per cent at room temperature and 1.0 per cent at the eutectoid temperature, 820°C.  $\beta$ -manganese did not dissolve large amount of carbon, the maximum solubility being 0.05 per cent at 857°C.  $\gamma$ -manganese dissolved a comparatively large amount of carbon. Solubility of carbon in  $\delta$ -manganese was comparatively small, being only 0.12 per cent at 1235°C.

(7)  $\alpha$ C solid solution was newly discovered in the present study, which existed in the alloys containing more than 7.0 per cent of carbon. This seemed to be the solid solution of manganese carbide  $Mn_2C$  (9.85% C) dissolving manganese. In this binary system, the manganese carbide  $Mn_3C$  which had been expected to exist, was not actually observable and merely corresponded to the phase boundary of  $\alpha$ C solid solution at lower carbon side.

(8)  $\beta$ C solid solution appeared in the alloys containing more than 3.05 per cent of carbon at high temperatures. The solubility of carbon was 3.05 and 8.4 per cent at 950 and 1340°C, respectively.  $\beta$ C state obtained by quenching was comparatively stable, compared with other states. Hence, in the alloys of the state of  $\beta$ C solid solution, the weathering phenomenon was hardly observable, whereas, in the case of an alloy containing higher percentage of carbon, fine powders due to weathering disintegration were easily produced.

(9)  $\gamma$ C solid solution was also newly recognized by the present study. This phase was produced by the peritectoid reaction at 1010°C, and its composition corresponded to the carbide  $Mn_4C$  (5.18% C). The range of existence of  $\gamma$ C solid solution at room temperature was from 4.3 to 4.6 per cent of carbon.

(10) The equilibrium diagram of pure manganese and carbon system was

completely established for the first time.

#### **Aknowledgement**

In conclusion, the present writer wishes to express his hearty thanks to Dr. T. Ishiwara, the ex-Director of the Research Institute for Iron, Steel and Other Metals, under whose direction the present study was carried out, and also to Mr. T. Numata for his zealous assistance during this study and to Dr. A. Osawa and Mr. T. Murata for the X-ray analysis.